RSC Advances

PAPER

View Article Online
View Journal | View Issue

Open Access Article. Published on 03 April 2023. Downloaded on 10/28/2025 2:01:20 AM.
This article is licensed under a Creative Commons Attribution-NonCommercial 3.0 Unported Licence.

Check for updates

Cite this: *RSC Adv.*, 2023, **13**, 10488

Design, synthesis, anticancer evaluation, and *in silico* ADMET analysis of novel thalidomide analogs as promising immunomodulatory agents†

Anas Ramadan Kotb,[a] Abdallah E. Abdallah,[a]* Hazem Elkady,[a]* Ibrahim H. Eissa,[a] Mohammed S. Taghour,[a] Dina Abed Bakhotmah,[b] Tamer M. Abdelghany[cd] and Mohamed Ayman El-Zahabi*[a]

Immunomodulatory medications like thalidomide and its analogs prevent the production of some proinflammatory cytokines linked to cancer. A new series of thalidomide analogs were designed and synthesized in order to develop potential antitumor immunomodulatory agents. The antiproliferative activities of the new candidates against a panel of three human cancer cell lines (HepG-2, PC3 and MCF-7) were assessed in comparison to thalidomide as a positive control. The obtained results showed the relative significant potency of **18f** (IC_{50} = 11.91 ± 0.9, 9.27 ± 0.7, and 18.62 ± 1.5 μM) and **21b** (IC_{50} = 10.48 ± 0.8, 22.56 ± 1.6, and 16.39 ± 1.4 μM) against the mentioned cell lines, respectively. These results were comparable to thalidomide (IC_{50} = 11.26 ± 0.54, 14.58 ± 0.57, and 16.87 ± 0.7 μM, respectively). To see to what extent the biological properties of the new candidates are relative to those of thalidomide, the effects of **18f** and **21b** on the expression levels of TNF-α, CASP8, VEGF, and NF-κB P65 were evaluated. Significant reductions in the proinflammatory TNF-α, VEGF, and NF-κB P65 levels in HepG-2 cells were observed after exposure to compounds **18f** and **21b**. Furthermore, a sharp increase in CASP8 levels was detected. The obtained results revealed that **21b** is of greater significance than thalidomide in TNF-α and NF-κB P65 inhibition. The *in silico* ADMET and toxicity studies showed that most of tested candidates have a good profile of drug-likeness and low toxicity potential.

Received 4th January 2023
Accepted 27th March 2023

DOI: 10.1039/d3ra00066d

rsc.li/rsc-advances

1. Introduction

Immunomodulatory drugs modify the response of the immune system by increasing (immunostimulants) or decreasing (immunosuppressives) the production of serum antibodies.[1] Immunostimulant drugs are prescribed to enhance the immune response against infectious diseases, tumors, primary or secondary immunodeficiency, and alterations in antibody transfer, among others.[2] Immunosuppressive drugs are used to reduce the immune response against transplanted organs and to treat autoimmune diseases such as pemphigus, lupus, or allergies.[3] In contrast to immunosuppressive agents that inhibit the immune response in transplant rejection and autoimmunity, a few immunostimulatory drugs have been developed with applicability to infection, immunodeficiency, and cancer. Problems with such drugs include systemic (generalized) effects at one extreme or limited efficacy at the other.[3]

Thalidomide **I**, lenalidomide **II**, and pomalidomide **III** are a class of immunomodulatory drugs that contain imide groups targeting cereblon (CRBN). These drugs work through various mechanisms of actions that promote malignant cell death and enhance host immunity.[4,5] Thalidomide is considered as a prototype of the glutarimide-containing immunomodulatory agents.[6] It inhibits the production of many proinflammatory mediators such as tumor necrosis factor-alpha (TNF-α) and can affect the production of others, such as interleukin-1b (IL-1b), IL-2, IL-4, IL-5, IL-6, IL-10, and interferon-γ (IFN-γ).[7] Moreover, thalidomide and its analogs inhibit the secretion of both beta fibroblast growth factor (bFGF) and vascular endothelial growth factor (VEGF) from cancer cells and bone marrow stromal cells, leading to reduction of endothelial cell migration and proliferation and induction of apoptosis.[8]

Second-generation thalidomide analogs, lenalidomide **II**, is a potent immunomodulator that is 50 000 times more potent than thalidomide as an inhibitor of TNF-α.[9] Clinical studies have revealed that lenalidomide demonstrates fewer side effects

[a]*Pharmaceutical Medicinal Chemistry & Drug Design Department, Faculty of Pharmacy (Boys), Al-Azhar University, Cairo, 11884, Egypt. E-mail: Abdulla_emara@azhar.edu.eg; Hazemelkady@azhar.edu.eg; malzahaby@azhar.edu.eg*

[b]*Department of Chemistry, Faculty of Science, King Abdulaziz University, Jeddah, Saudi Arabia*

[c]*Department of Pharmacology& Toxicology, Faculty of Pharmacy, Al-Azhar University, Cairo, Egypt*

[d]*Department of Pharmacology& Toxicology, Faculty of Pharmacy, Heliopolis University for Sustainable Development, Cairo, Egypt*

† Electronic supplementary information (ESI) available. See DOI: https://doi.org/10.1039/d3ra00066d

© 2023 The Author(s). Published by the Royal Society of Chemistry

Open Access Article. Published on 03 April 2023. Downloaded on 10/28/2025 2:01:20 AM.
This article is licensed under a Creative Commons Attribution-NonCommercial 3.0 Unported Licence.

and almost neither neurological toxicity nor teratogenicity, compared to thalidomide.[10] Structural modification of thalidomide *via* the addition of an amino group at the 4-position of the phthaloyl ring forming pomalidomide **III** which was 10-fold more potent than lenalidomide as a TNF-α inhibitor and interleukin-2 (IL-2) stimulator.[11] It also showed better anti-angiogenic results than thalidomide and lenalidomide.[12]

Great attention has focused on the possible use of thalidomide as an anti-angiogenic agent – a property that might account for its teratogenicity. The ability of a tumor to induce new blood vessel formation is crucial for the growth of solid tumors and for metastasis. The similarities between this process in the promotion of tumor growth and in chronic inflammation supports a possible role for thalidomide in the treatment of cancers. There are reports of efficacy in patients with multiple myeloma[13] and thalidomide has been reported to possess anti-angiogenic properties.[14]

Other CRBN targeting thalidomide analogs were developed in an attempt to overcome the toxicity of thalidomide. These compounds include CC-122 (avadomide) **IV**, CC-220 (iberdomide) **V**, and CC-885 **VI**.[15] Avadomide is effective for the treatment of multiple myeloma and diffuse large B-cell lymphoma (DLBCL), whereas iberdomide is effective for systemic lupus erythematosus (SLE)[16] (Fig. 1). CC-885 was recently identified as CRBN modulator with potent activities against solid tumors.[17]

Three common pharmacophoric features of thalidomide and its analogs can be identified, as is presented in Fig. 1. These features include: (i) aromatic domain, (ii) spacer, and (iii) glutarimide moiety. In this work, we designed and synthesized a new series of anticancer agents having the same essential pharmacophoric features of thalidomide.

1.1. Rationale of molecular design

Forcing by all mentioned facts and the promising findings obtained in our former work,[18] we decided to start the present work. The rational of molecular design depended on ligand-based drug design approach to develop potent thalidomide analogs. In line with the pharmacophoric features of thalidomide and on the basis of the structural features of potent thalidomide analogs, we made modifications on thalidomide structure (Fig. 2). It can be noticed that the modifications were at three different sites including the aromatic ring system, the linker, and the glutarimide moiety.

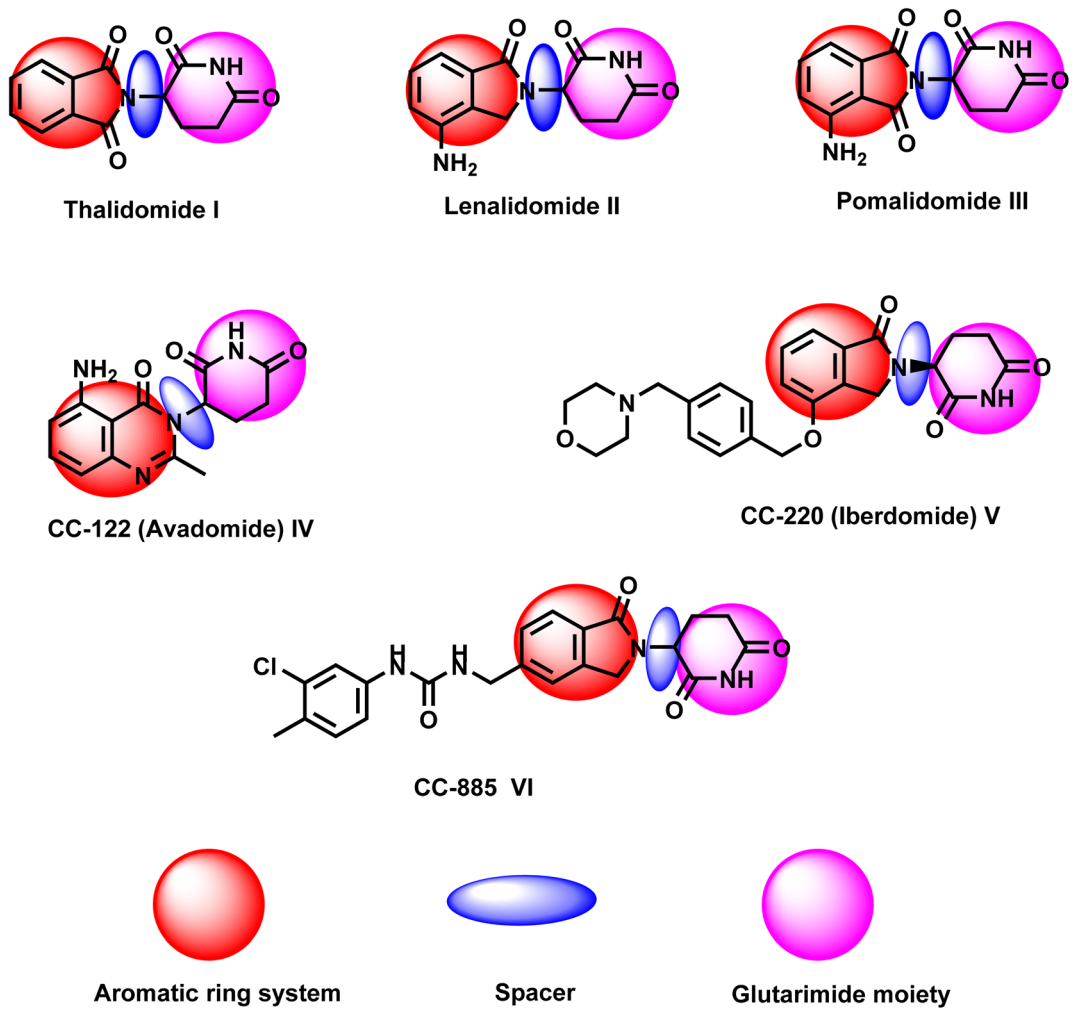

Fig. 1 Reported thalidomide analogs having the same pharmacophoric features.

Open Access Article. Published on 03 April 2023. Downloaded on 10/28/2025 2:01:20 AM.
This article is licensed under a Creative Commons Attribution-NonCommercial 3.0 Unported Licence.

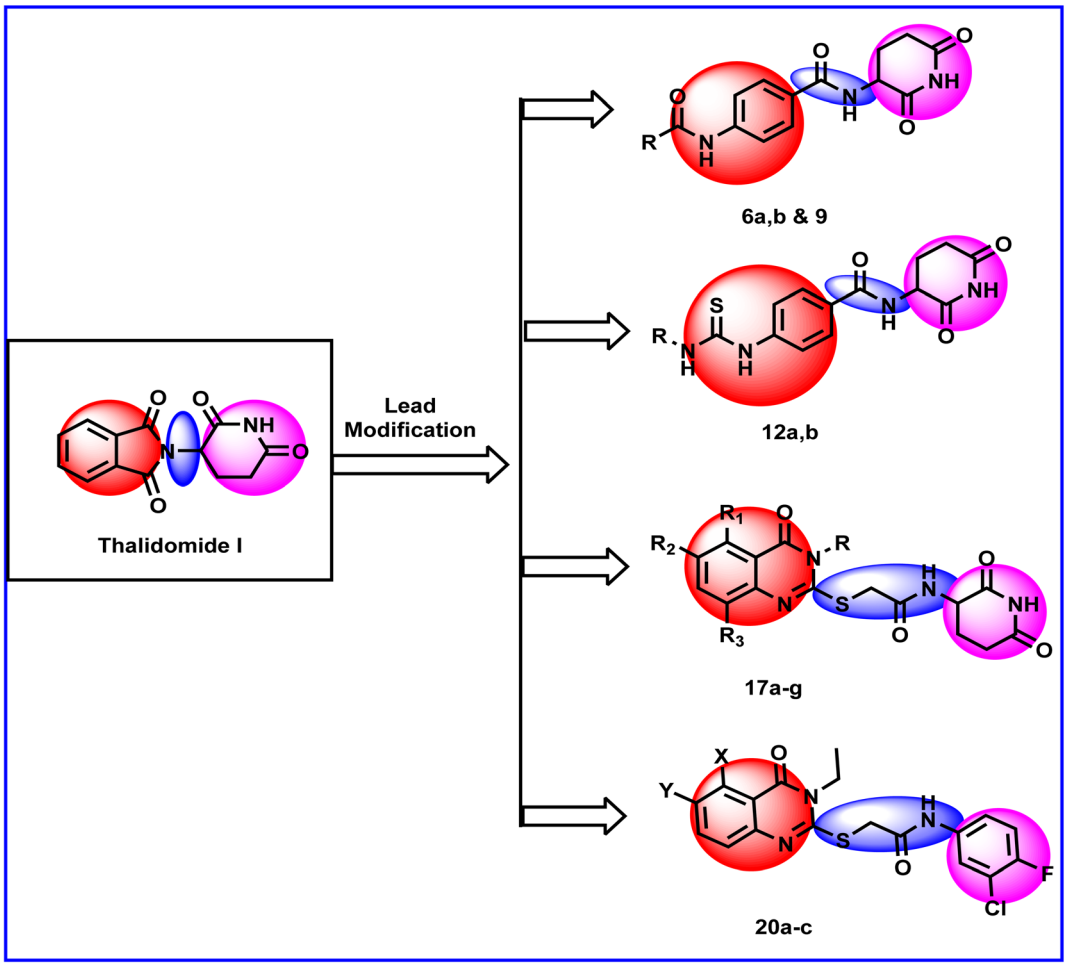

Fig. 2 Rationale of the work using thalidomide as lead compound.

Initially, different aromatic systems extracted from potent thalidomide analogs of significant clinical characteristics have been designed. Similar to avadomide, compounds **17a–g** and **20a–c** were based on quinazolinone. Meanwhile, substituted phenylthiourea moiety was constructed in compound **12** as a bio-isostere to phenylurea moiety presented in CC-885. Furthermore, anilide group was introduced in compounds **6a,b** and **9** as can be seen in Fig. 2.

With respect to the linker, we can see amide group in compounds **6a,b**, **9**, and **12** and thioacetamide in compounds **17a–g** and **20a–c**. The two linkers were of different lengths to study the effect of the distance between the aromatic system and the glutarimide moiety on the activity. At the same time, the new linkers had two or three bonds of free rotation, which would contribute to the flexibility of the new molecules relative to thalidomide which contains a one bond linker with restricted rotation.

Regarding the glutarimide moiety, it was kept as it is in all the designed members, whereas it was only replaced with 3-chloro-4-fluorophenyl moiety in compounds **20a–c**. Variability of the substitutions enabled us to study the structure–activity relationships of the final compounds as a main objective of this work (Fig. 2).

The antiproliferative activities of synthesized compounds were assessed against three cancer cell lines namely; hepatocellular carcinoma (HepG-2), prostate carcinoma (PC3), and breast cancer (MCF-7). The immunomodulatory activities of the synthesized compounds were evaluated against different enzymes including caspase-8, VEGF, NFκB P65, and TNF-α. Furthermore, the kinetic and toxicity profile of the synthesized compounds were assessed *in silico*.

2. Results and discussion

2.1. Chemistry

According to the above rationale, Schemes 1–4 were carried out for furnishing the target compounds **6a,b**, **9**, **12**, **18a–g**, and **21a–c**.

Compounds **3a,b** were synthesized according to the reported method which involves addition of the appropriate anhydride to 4-aminobenzoic acid in pyridine at r.t.[19] Pyridine was a suitable solvent because it is of p*K*a 5.2. It is a stronger base than the amino group of 4-aminobenzoic acid which has p*K*a of 2.7. Hence, pyridinium carboxylate salt will be formed instead of zwitter ion of 4-aminobenzoic acid increasing the availability of the lone pair of the amino group. At the same time, compound **8**

 © 2023 The Author(s). Published by the Royal Society of Chemistry

Open Access Article. Published on 03 April 2023. Downloaded on 10/28/2025 2:01:20 AM.
This article is licensed under a Creative Commons Attribution-NonCommercial 3.0 Unported Licence.

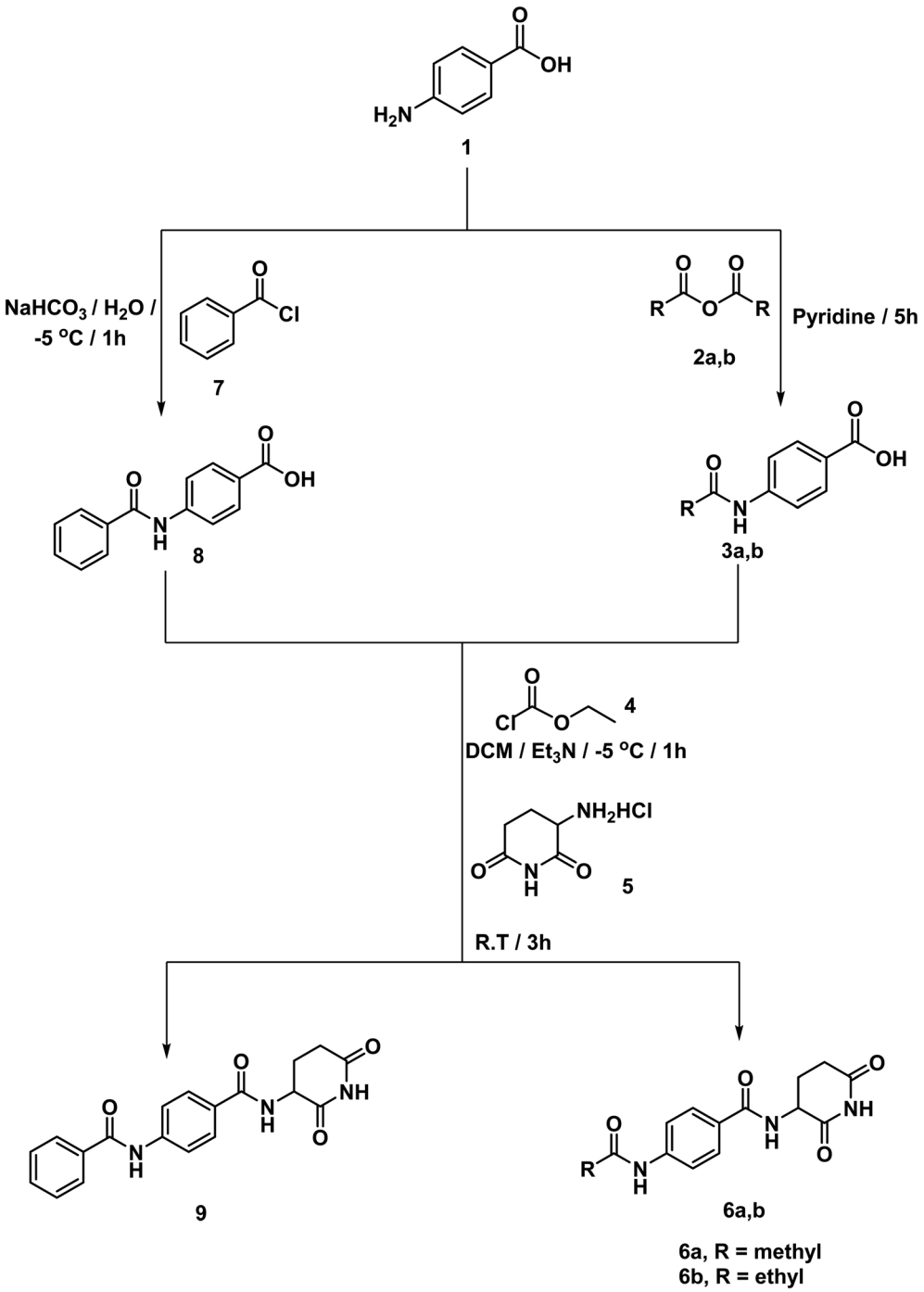

Scheme 1 Synthesis of compounds **6a,b**, and **9**.

was formed *via* drop wise addition of benzoyl chloride to an aqueous solution of sodium 4-aminobenzoate with stirring. Next, the target compound was furnished using mixed anhydride method that involved reaction of ethyl chloroformate with the carboxylic group of **3a,b**, and **8** to give the corresponding mixed anhydride in DCM. Then 3-aminopiperidine-2,6-dione was allowed to react with the formed anhydrides to furnish the target compounds **6a,b**, and **9**, respectively (Scheme 1). The structures of compounds **6a,b**, and **9** were verified by their elemental and spectral data. The IR spectra of this series revealed the presence of imide carbonyl absorption bands at a range of 1690 to 1730 cm^{-1}, amide carbonyl absorption bands at a range of 1645 to 1680 cm^{-1} and presence of NH bands at a range of 3176–3368 cm^{-1}. On the other hand, the ^1H NMR spectra showed peaks at about 10.85, 10.3 and 8.6 ppm for imidic NH and the two amidic NH, respectively. Moreover, their ^1H NMR spectra revealed the signals of the aliphatic NCH and CH_2CH_2CO proton at a range of 4.79–4.72 and 2.61–1.92 ppm, respectively for the introduced glutarimide ring.

Open Access Article. Published on 03 April 2023. Downloaded on 10/28/2025 2:01:20 AM.
This article is licensed under a Creative Commons Attribution-NonCommercial 3.0 Unported Licence.

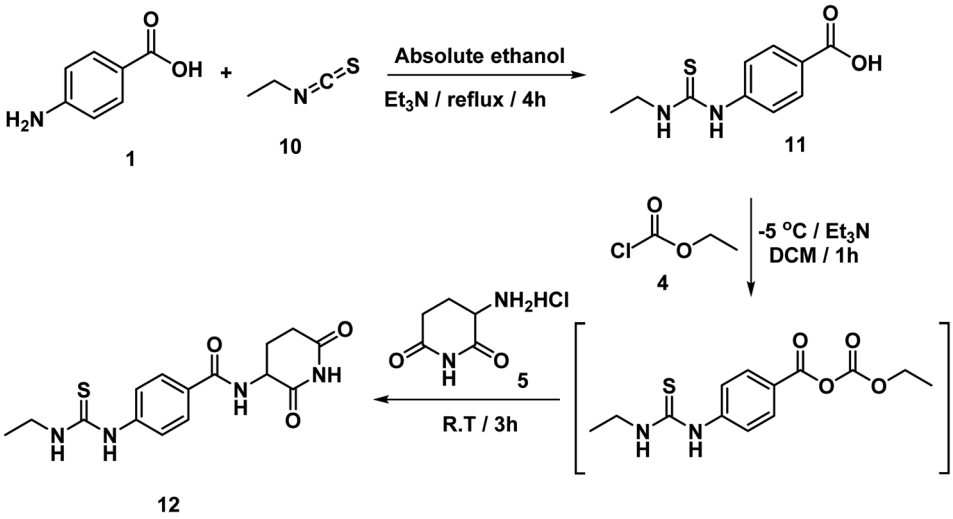

Scheme 2 Synthesis of compounds 12.

The intermediate compounds **11a,b** were synthesized by refluxing 4-aminobenzoic acid with the proper isothiocyanates in ethanol in the presence of Et_3N. In this reaction, the nucleophilic amino group of 4-aminobenzoic acid attacked the electron deficient carbon of isothiocyanates. Then compound **12** was synthesized in line with a reported mixed anhydride method[20,21] by reaction of 4-(3-ethylthioureido)benzoic acid **11** with ethyl chloroformate in the presence of Et_3N followed by 3-aminopiperidine-2,6-dione (Scheme 2). The structure of compound **12** was verified by its elemental and spectral data. The IR spectrum revealed the presence of imide carbonyl and amide carbonyl absorption band at 1726. On the other hand, the ^{1}H NMR spectrum of compound **12** showed peaks at about 10.85, 10.3 and 8.3 ppm for imidic NH and the two amidic NH, respectively. Moreover, the ^{1}H NMR spectrum revealed the signals of the aliphatic NCH and CH_2CH2CO proton at a range

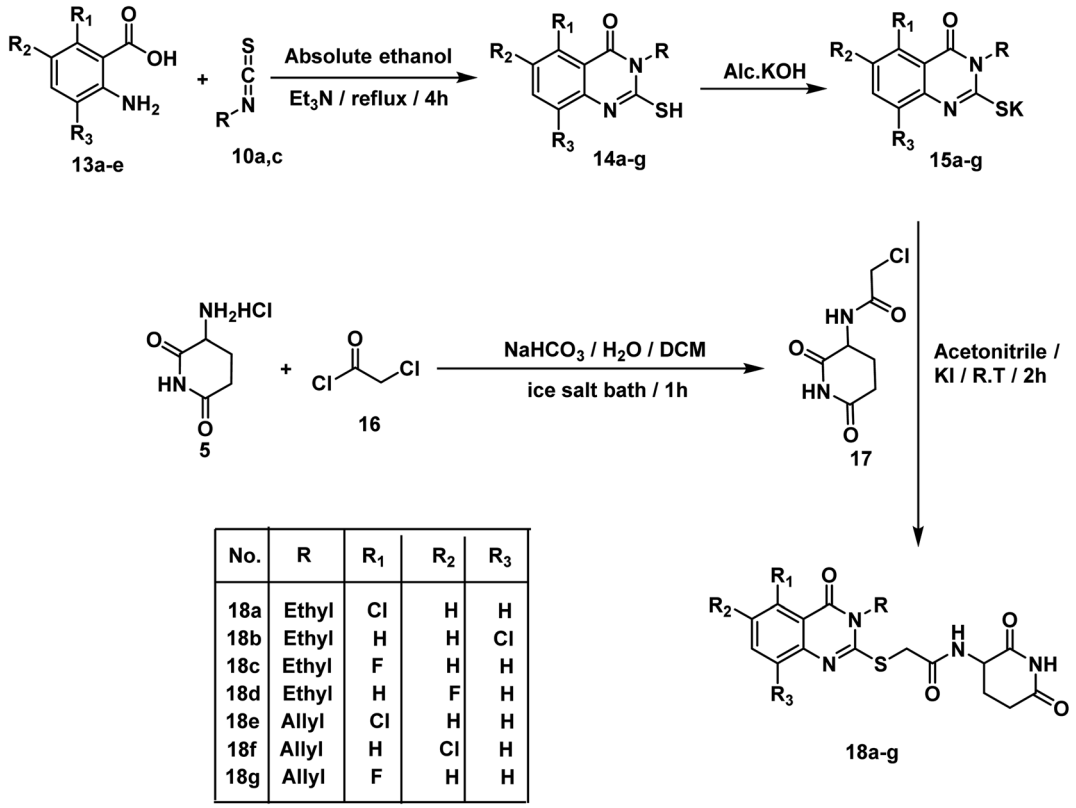

No.	R	R_1	R_2	R_3
18a	Ethyl	Cl	H	H
18b	Ethyl	H	H	Cl
18c	Ethyl	F	H	H
18d	Ethyl	H	F	H
18e	Allyl	Cl	H	H
18f	Allyl	H	Cl	H
18g	Allyl	F	H	H

Scheme 3 Synthesis of compounds 18a–g.

 © 2023 The Author(s). Published by the Royal Society of Chemistry

Open Access Article. Published on 03 April 2023. Downloaded on 10/28/2025 2:01:20 AM.
This article is licensed under a Creative Commons Attribution-NonCommercial 3.0 Unported Licence.

of 4.77 and 2.80–2.56 ppm, respectively for the introduced glutarimide ring.

In accordance with the reported method, we prepared compounds **14a–g**. This method involves refluxing an appropriate anthranilic acid derivative namely; 6-chloroanthranilic acid **13a**, 3-chloroanthranilic acid **13b**, 6-fluoroanthranilic acid **13c**, 5-fluoroanthranilic acid **13d**, and 5-chloroanthranilic acid **13e** with the appropriate isothiocyanates namely; ethyl isothiocyanate **10a** or allyl isothiocyanate **10c** in absolute ethanol and in the presence of Et_3N.[22,23] The potassium salts **15a–g** were furnished *via* heating the appropriate 2-mercaptoquinazolin-4-one derivatives **14a–g** with equimolar amount of KOH in ethanol.[23] On the other hand, compound **16** was produced in two phase system (DCM and water) in the presence of two molar equivalent of $NaHCO_3$ in ice-salt bath as reported. Then, we obtained the final compounds **18a–g** in good yields by stirring the appropriate mercapto salt of quinazoline derivatives **15a–g** with the chloroacetamide derivative **16** and KI at r.t. in acetonitrile (Scheme 3). The structures of compounds **15a–g** were verified by their elemental analyses and spectral data. The IR charts of compounds **15a–g** showed bands for imide CO of glutarimide ring at about 1708 to 1720 cm^{-1}. While amide CO showed bands from 1623 to 1684 cm^{-1}. On the other hand, the ^1H NMR spectra of compounds **15a–g** showed peaks at about 10.8 and 8.6 ppm for imide NH and amide NH, respectively. Methylene protons flanked between sulfur and carbonyl appeared as a singlet peak at about 4.1 ppm.

The acetamide derivative **20** was obtained by addition of chloroacetyl chloride **16** to a mixture of 3-chloro-4-fluoroaniline **19** and $NaHCO_3$ in DMF in ice salt bath. Stirring the appropriate mercapto salt of quinazoline derivatives **15a–g** with the acetamide derivative **20** and KI at r.t. in acetonitrile afforded the final compounds **21a–c** in good yields (Scheme 4). The ^1H NMR spectra showed peaks at about 10.69 and 10.74 ppm for amide NH. Methylene protons flanked between sulfur and carbonyl appeared as a singlet peak at about 4.2 ppm.

2.2. Biological testing

2.2.1. *In vitro* anti-proliferative activity. It was reported that some types of cancer have a high incidence and mortality rate. Among which are breast, liver, and prostate cancers.[24] MTT method was used to evaluate the anti-proliferative activities of compounds **6a,b**, **9**, **12**, **18a–g**, and **21a–c** against three cancer cell lines namely: hepatocellular carcinoma (HepG-2), prostate carcinoma (PC3), and breast cancer (MCF-7). Thalidomide was examined as a positive control. The MTT results presented in Table 1 reflects the variability in activity towards the tested cell lines. It can be noticed that Compounds **18f** ($IC_{50} = 11.91 \pm 0.9$, 9.27 ± 0.7, and 18.62 ± 1.5 μM against HepG-2, PC3, and MCF-7, respectively) and **21b** ($IC_{50} = 10.48 \pm 0.8$, 22.56 ± 1.6, and 16.39 ± 1.4 μM against HepG-2, PC3, and MCF-7, respectively) exhibited the most promising anti-proliferative activities among all the tested members. These values were comparable to those of thalidomide ($IC_{50} = 11.26 \pm 0.54$, 14.58 ± 0.57, and 16.87 ± 0.7 μM against HepG-2, PC3, and MCF-7, respectively). Moreover, compounds as **12**, **18a**, **18c**, and **18g** revealed good anti-proliferative activities against the tested cell lines with IC_{50} values ranging from 12.13 to 37.95 μM. On the other hand, the

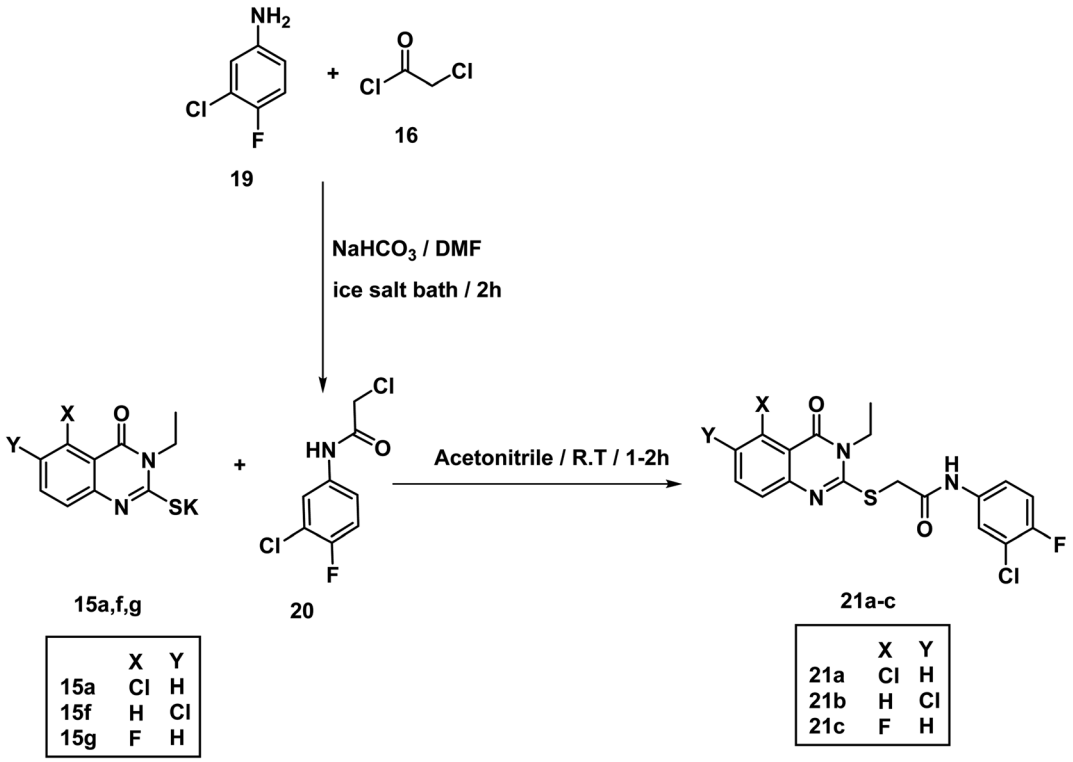

Scheme 4 Synthesis of compounds 21a–c.

Open Access Article. Published on 03 April 2023. Downloaded on 10/28/2025 2:01:20 AM.
This article is licensed under a Creative Commons Attribution-NonCommercial 3.0 Unported Licence.

Table 1 Anti-proliferative activities of the target compounds against HepG-2, PC3 and MCF-7 cell lines

	In vitro cytotoxicity IC_{50} (μM) [a]		
Comp.	HepG-2	PC3	MCF-7
6a	49.34 ± 3.4	39.27 ± 2.7	65.27 ± 3.6
6b	62.78 ± 3.8	48.02 ± 3.1	56.39 ± 3.3
9	53.39 ± 3.6	57.48 ± 3.4	78.25 ± 4.4
12	37.22 ± 2.6	25.91 ± 1.9	34.81 ± 2.5
18a	18.90 ± 1.4	32.86 ± 2.3	37.95 ± 2.5
18b	39.76 ± 2.6	60.29 ± 3.6	49.70 ± 2.9
18c	33.82 ± 2.2	12.13 ± 1.1	26.89 ± 2.1
18d	72.31 ± 3.9	82.38 ± 4.3	93.16 ± 4.8
18e	42.65 ± 3.1	31.36 ± 2.4	64.03 ± 3.4
18f	11.91 ± 0.9	9.27 ± 0.7	18.62 ± 1.5
18g	30.23 ± 2.3	23.04 ± 1.9	36.18 ± 2.7
21a	52.47 ± 3.1	39.94 ± 2.7	61.51 ± 3.3
21b	10.48 ± 0.8	22.56 ± 1.6	16.39 ± 1.4
21c	55.02 ± 3.2	67.72 ± 3.9	79.05 ± 4.0
Thalidomide	11.26 ± 0.54	14.58 ± 0.57	16.87 ± 0.7

[a] Three independent experiments were performed for each concentration.

rest of the compounds displayed moderate anti-proliferative activities against the tested cell lines.

2.2.2. Structure activity relationship. From the aforementioned *in vitro* anti-proliferative activity findings, we could conclude appreciated information about the structure–activity relationships (Fig. 3).

Regarding 3-ethyl-2-substitutedquinazolin-4-one containing derivatives; 5-fluoro candidate **18c** (IC_{50} = 33.82 ± 2.2, 12.13 ± 1.1, and 26.89 ± 2.1 μM against HepG-2, PC3, and MCF-7, respectively) was more potent than the corresponding 6-fluoro one **18d** (IC_{50} = 72.31 ± 3.9, 82.38 ± 4.3, and 93.16 ± 4.8 μM against HepG-2, PC3, and MCF-7, respectively) against all cell lines. Moreover, 5-chloro derivative **18a** (IC_{50} = 18.90 ± 1.4, 32.86 ± 2.3, and 37.95 ± 2.5 μM against HepG-2, PC3, and MCF-7, respectively) was more potent than the corresponding 8-chloro one **18b** (IC_{50} = 39.76 ± 2.6, 60.29 ± 3.6, and 49.70 ± 2.9 μM against HepG-2, PC3, and MCF-7, respectively) against all cell lines. For 3-ally-2-substitutedquinazolin-4-derivatives, it was noticed that 6-chloro counterpart **18f** (IC_{50} = 11.91 ± 0.9, 9.27 ± 0.7, and 18.62 ± 1.5 μM against HepG-2, PC3, and MCF-7, respectively) was more advantageous than 5-fluoro analog **18g** (IC_{50} = 30.23 ± 2.3, 23.04 ± 1.9, and 36.18 ± 2.7 μM against HepG-2, PC3, and MCF-7, respectively). However, the 5-chloro containing derivative **18e** (IC_{50} = 42.65 ± 3.1, 31.36 ± 2.4, and 64.03 ± 3.4 μM against HepG-2, PC3, and MCF-7, respectively) displayed less potent inhibitory activity against the tested cell lines.

Comparing the cytotoxic activity of compounds **21a–c** (quinazoline derivatives containing 3-chloro-4-fluorophenyl moieties) indicated that 6-chloro **21b** is more preferred biologically than 5-chloro **21a** and 5-fluoro **21c** members against all cell lines.

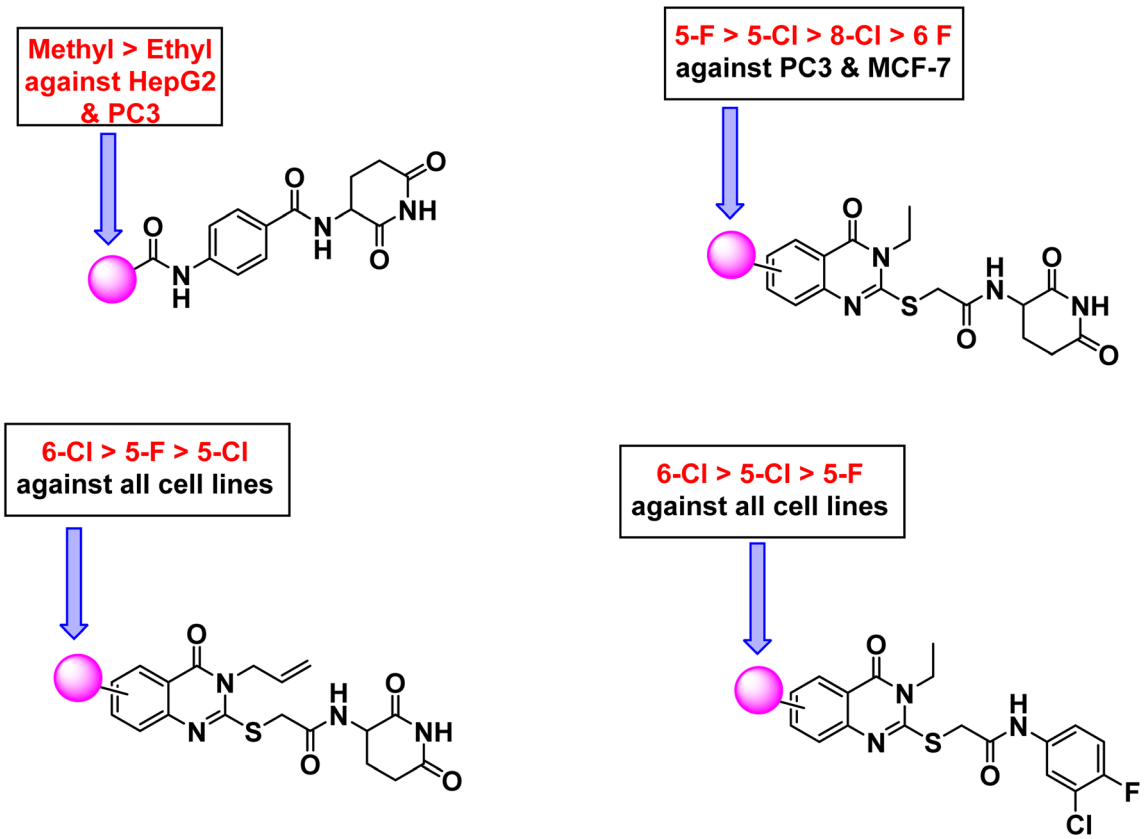

Fig. 3 SAR of the synthesized members.

 © 2023 The Author(s). Published by the Royal Society of Chemistry

Open Access Article. Published on 03 April 2023. Downloaded on 10/28/2025 2:01:20 AM. This article is licensed under a Creative Commons Attribution-NonCommercial 3.0 Unported Licence.

Table 2 The effect of compounds **18f**, **21b**, and thalidomide on the levels of CASPASE-8

Comp. no.	CASPASE-8 (ng mL^{-1})
18f	6.7
21b	6.5
Control	1.08
Thalidomide	8.3

2.2.3. *In vitro* immunomodulatory assay. The effects of compounds **18f** and **21b** on the expression levels of caspase-8, VEGF, NFκB P65, and TNF-α were examined in HepG-2 cells along with thalidomide as a positive control.

2.2.3.1. The effect on the expression level of caspase-8. As presented in Table 2, thalidomide and compounds **18f** and **21b** showed a statistically significant increase in caspase-8 levels compared with control cells. Also, it was found that compounds **18f** and **21b** were able to increase caspase-8 level in HepG-2 cells by 6.7 and 6.5 ng mL^{-1}, respectively, compared to 8.3 ng mL^{-1} for thalidomide.

2.2.3.2. The effect on the expression level of vascular endothelial growth factor (VEGF). The data presented in Table 3 showed that thalidomide and compounds **18f** and **21b** showed a significant decrease in VEGF level comparing with control cells. HepG-2 cells treated with **18f** and **21b** revealed VEGF level of 169.6 and 162.3 pg mL^{-1}, respectively, compared to 153.2 pg mL^{-1} calculated for thalidomide.

2.2.3.3. The effect on NF-κB P65 expression level. The obtained data indicated that the impact of **18f** and **21b** on NF-κB P65 were much better than thalidomide. It can be seen that NF-κB P65 level in HepG-2 cells treated with **18f** and **21b** were 89.4 and 85.1 pg mL^{-1} compared to 110.5 pg mL^{-1} measured for thalidomide treated HepG-2 cells. At the same time, the two tested compounds showed a significant decrease in NF-κB P65 levels when compared to control treated cells (Table 4).

Table 3 The effect of compounds **18f**, **21b**, and thalidomide on the levels of VEGF

Comp. no.	VEGF (pg mL^{-1})
18f	169.6
21b	162.3
Control	432.5
Thalidomide	153.2

Table 4 The effect of compounds **18f**, **21b**, and thalidomide on the levels of NFκB P65

Compound	NFκB P65 (pg mL^{-1})
18f	89.4
21b	85.1
Control	278.1
Thalidomide	110.5

Table 5 The effect of compounds **18f**, **21b**, and thalidomide on the levels of TNF-α

Compound	TNF-α (pg mL^{-1})
18f	73.2
21b	50.6
Control	162.5
Thalidomide	53.1

2.2.3.4. The effect on TNF-α expression level. The data presented in Table 5 shows that both **18f** and **21b** significantly reduced TNF-α levels in HepG-2 cells. TNF-α levels were reduced from 162.5 pg mL^{-1} in control cells to 73.2 and 50.6 pg mL^{-1} under the effects of **18f** and **21b** respectively. Meanwhile, the level in cells treated with thalidomide was 53.1 pg mL^{-1}. These findings highlight the importance of **21b** as TNF-α inhibitor in comparison with thalidomide.

2.2.3.5. HepG-2 cell cycle analysis. The most promising candidate, compound **21b**, was further evaluated by analyzing its effect on cycle phases of the HepG-2 cells. From the results presented in Table 6, it can be noticed that a large percentage (54.05%) of cells treated with **21b** was accumulated at G0/G1 phase compared to 8.07 and 10.05% reported for thalidomide and control cells, respectively. This clearly indicates the ability of compound **21b** to inhibit HepG-2 cell proliferation efficiently at G0/G1 phase (Fig. 4).

*2.2.3.6. The effect of **21b** on apoptosis and necrosis rates of HepG-2.* As presented in Table 7 and Fig. 5, the death rate of HepG-2 cells treated with compound **21b** dramatically increased from 1.19% to 25.78% at the early stage of apoptosis. Meanwhile, there is no significant increase in the late apoptosis and necrosis. This suggests that apoptosis was the main mechanism of HepG-2 cell death that was caused by compound **21b**.

2.2.4. ADMET profiling study. *In silico* studies are preferred for a variety of reasons, including the restrictions on cost, time, and effort as well as the strict laws regarding animal testing.[25,26] Although there are many *in vitro* studies that can be carried out to investigate the properties of ADMET, they are not always the most effective method.[27,28] Therefore, the ADMET characteristics of the examined compounds were assessed computationally using Discovery Studio 4.0.[29–31] Thalidomide was used a reference.

The most promising candidates **18f** and **21b** show acceptable range of the expected ADMET profile. Compound **18f** was predicted to have low blood–brain barrier (BBB) penetration level. While compound **21b** was expected to have high penetration

Table 6 The impact of compound **21b** on HepG-2 cell cycle

Sample	G0/G1	S	G2/M
Control	10.05	59.55	29.73
Thalidomide	8.07	66.38	25.54
21b	54.05	37.04	8.96

Open Access Article. Published on 03 April 2023. Downloaded on 10/28/2025 2:01:20 AM.
This article is licensed under a Creative Commons Attribution-NonCommercial 3.0 Unported Licence.

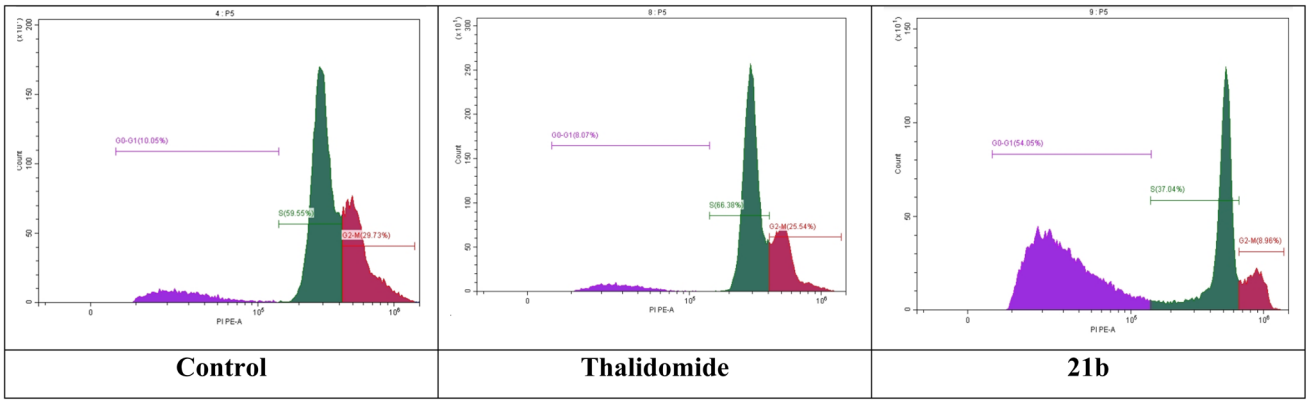

Fig. 4 The effect of **21b** on different phases of HepG-2 cell cycle.

Table 7 Effect of compound **21b** on apoptosis and necrosis rates of HepG-2 cells

Sample	Normal cells	Early apoptosis	Late apoptosis	Necrosis
Control	98.61	1.19	0.18	0.02
Thalidomide	95.98	3.76	0.26	0.00
21b	74.00	25.78	0.19	0.03

level. For aqueous solubility, compounds **18f** and **21b** showed good and low levels, respectively. It is noteworthy that compounds **18f** and **21b** have good absorption levels and do not inhibit CYP2D6. Regarding plasma protein binding parameter, compounds **18f** was anticipated to bind plasma protein less than 90% while **21b** was expected to bind it with more than 90% (Table 8 and Fig. 6).

2.2.5. *In silico* toxicity studies. Eight toxicity parameters were evaluated according to the toxicity models developed with the Discovery studio software. Thalidomide was used as a reference (Table 9).

For ames mutagenicity (A-M), skin irritancy (S-I), ocular irritancy (O-I) models, and developmental toxicity potential model (DTP), the most promising candidates **18f** and **21b** were predicted as non-mutagen (N-M), non-irritant (N-I), mild irritant (M), and non-toxic (N-T), respectively.

For carcinogenic potency TD_{50} rat model (C-P-TD_{50}), compound **21b** showed TD_{50} values of 71.894 g per kg body weight, which is higher than thalidomide (26.375). For rat maximum tolerated dose (R-M-T-D) model, compound **18f** and **21b** demonstrated values higher than that of thalidomide. Additionally, compounds **18f** and **21b** revealed oral LD_{50} (R-O-LD_{50}) and LOAEL (R-C-LOAEL) values lower than thalidomide.

3. Conclusion

Fourteen thalidomide analogs have been designed and synthesized for anticancer and immunomodulatory evaluation. The *in vitro* cytotoxicity results revealed that compounds **18f** (IC_{50} = 11.91 ± 0.9, 9.27 ± 0.7, and 18.62 ± 1.5 μM against HepG-2, PC3, and MCF-7, respectively) and **21b** (IC_{50} = 10.48 ± 0.8, 22.56 ± 1.6, and 16.39 ± 1.4 μM against HepG-2, PC3, and MCF-7, respectively) were the most potent members. Also, compounds as **12**, **18a**, **18c**, and **18g** displayed good antiproliferative activities against the tested cell lines with IC_{50}

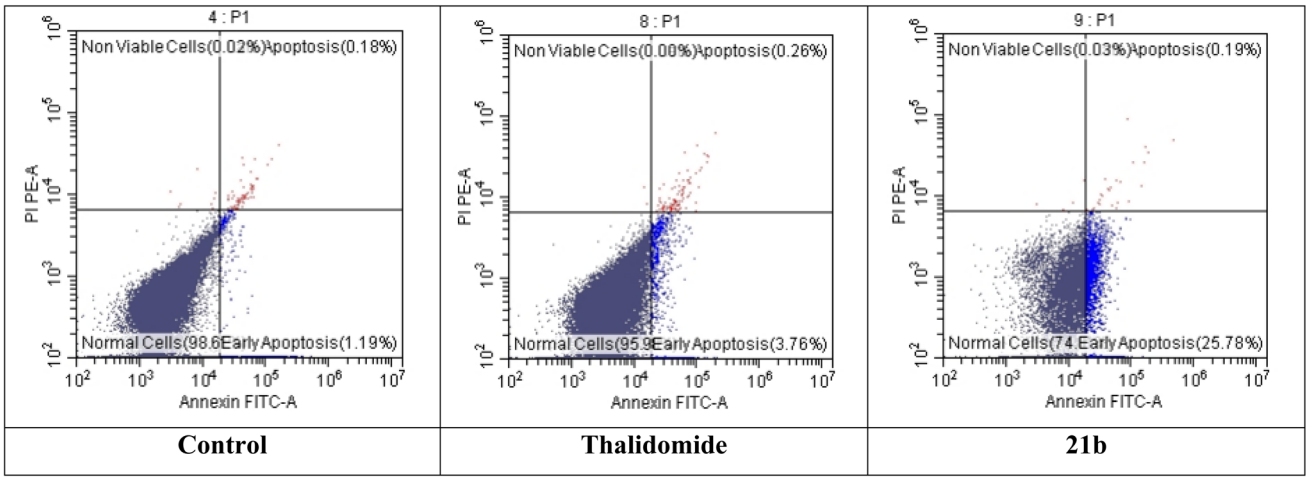

Fig. 5 Apoptosis and necrosis rates of HepG2 cells treated with **21b** compared to control and thalidomide.

 © 2023 The Author(s). Published by the Royal Society of Chemistry

Open Access Article. Published on 03 April 2023. Downloaded on 10/28/2025 2:01:20 AM.
This article is licensed under a Creative Commons Attribution-NonCommercial 3.0 Unported Licence.

Table 8 ADMET characteristics of the new candidates in comparison with thalidomide

Comp.	BBB level[a]	Solubility[b]	Absorption[c]	CYP2D6 inhibition[d]	Plasma protein binding[e]
6a	4	4	0	False	False
6b	3	4	0	False	False
9	3	3	0	False	False
12	3	3	0	False	False
18a	3	3	0	False	False
18b	3	3	0	False	False
18c	3	3	0	False	False
18d	3	3	0	False	False
18e	4	3	0	False	False
18f	4	3	0	False	False
18g	3	3	0	False	False
21a	1	1	0	False	True
21b	1	2	0	False	True
21c	1	1	0	False	True
Thalidomide	3	3	0	False	False

[a] 1 = high, 3 = low, and 4 = very low. [b] 1 = very low, 2 = low, 3 = good, and 4 = optimal. [c] 0 = good. [d] False = non inhibitor. [e] False means less than 90% & true means more than 90%.

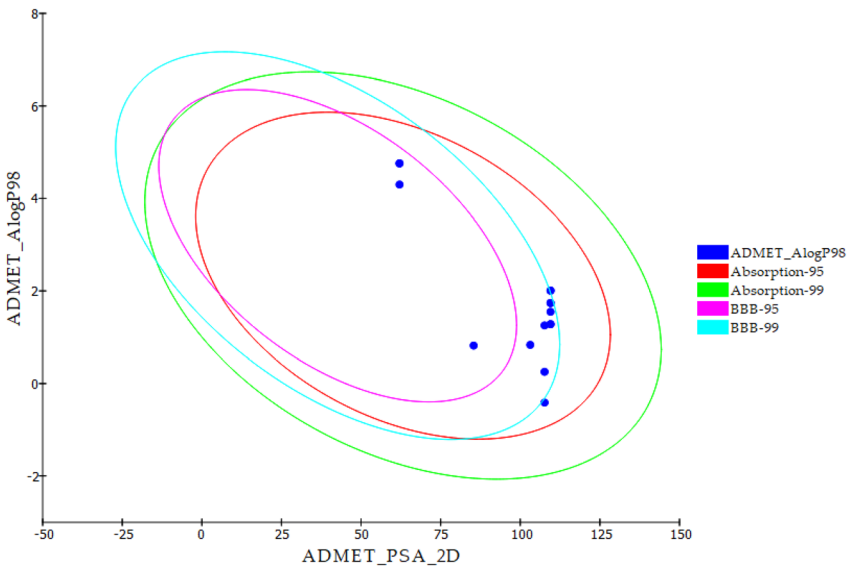

Fig. 6 ADMET properties of the new derivatives and thalidomide.

values ranging from 12.13 to 37.95 μM. Moreover, the most promising compounds **18f** and **21b** were further evaluated for their immunomodulatory effects. Compounds **18f** and **21b** showed a significant reduction in levels of TNF-α (from 162.5 pg mL^{-1} to 73.2 and 50.6 pg mL^{-1}), VEGF (from 432.5 pg mL^{-1} to 169.6 and 162.3 pg mL^{-1}), and NF-κB p65 (from 278.1 pg mL^{-1} to 89.4 and 85.1 pg mL^{-1}). Furthermore, compounds **18f** and **21b** exhibited significant elevation in CASP8 levels (from 1.08 ng mL^{-1} to 6.7 and 6.5 ng mL^{-1}). These results were compared to thalidomide as a reference standard which reports 53.1, 153.2, 110.5 pg mL^{-1} and 8 ng mL^{-1} against TNF-α, VEGF, NF-κB p65, and CASP8, respectively. The obtained findings suggest that the designed members have the potential to function as powerful immunomodulators and anticancer agents. Further optimization of these derivatives may lead to the discovery of more promising immunomodulatory agents.

4. Experimental

4.1. Chemistry

4.1.1. General procedure for synthesis of compounds 6a,b, and 9. Et_3N (0.18 mL, 1.20 mmol) was added to a suspension of the appropriate acid **3a,b**, and **8** (1.00 mmol) in DCM (15 mL) with stirring to give a clear solution. The reaction mixture was stirred in ice-salt bath for 5 min. Then ethyl chloroformate (0.10 mL, 1.05 mmol) was added dropwise over a period of 20 min. The reaction mixture was stirred for further 1 h at the same temperature. A solution of 3-aminopiperidine-2,6-dione HCl (0.17 g, 1.00 mmol) and triethyl amine (0.18 mL, 1.20 mmol) in DCM (10 mL) was added to the reaction mixture. The reaction mixture was stirred at r.t. for 3 h. After the reaction was complete (monitored by TLC), the impurities were removed by partitioning the organic layer with acidified water then with

Open Access Article. Published on 03 April 2023. Downloaded on 10/28/2025 2:01:20 AM.
This article is licensed under a Creative Commons Attribution-NonCommercial 3.0 Unported Licence.

Table 9 Evaluation of some toxicity parameters of the new synthesized compounds compared with thalidomide

Comp.	C-P-TD$_{50}$ (rat) [a]	A-M	R-M-T-D (feed) [b]	R-O-LD$_{50}$ [b]	R-C-LOAEL[b]	S-I	O-I	DTP
6a	2.890	N-M	0.107	5.079	0.171	N-I	M	T
6b	2.827	N-M	0.119	5.002	0.107	N-I	M	T
9	8.040	N-M	0.115	2.375	0.134	N-I	M	T
12	10.821	N-M	0.220	3.375	0.071	N-I	M	T
18a	2.240	N-M	0.055	1.287	0.023	N-I	M	N-T
18b	1.665	N-M	0.055	2.222	0.029	N-I	M	N-T
18c	2.397	N-M	0.059	0.673	0.024	N-I	M	N-T
18d	0.908	N-M	0.059	1.205	0.023	N-I	M	N-T
18e	5.760	N-M	0.055	0.564	0.007	N-I	M	N-T
18f	2.182	N-M	0.055	0.692	0.007	N-I	M	N-T
18g	6.173	N-M	0.059	0.295	0.007	N-I	M	N-T
21a	67.057	N-M	0.058	0.660	0.029	N-I	M	N-T
21b	71.894	N-M	0.062	0.693	0.029	N-I	M	N-T
21c	25.404	N-M	0.058	0.484	0.025	N-I	M	N-T
Thalidomide	26.375	N-M	0.047	0.835	0.133	N-I	None	N-T

[a] Unit: mg per kg body weight per day. [b] Unit: g per kg body weight.

$NaHCO_3$ aqueous solution. Upon evaporation, the organic solvent the obtained solid was washed with water then methanol to afford the corresponding benzamide derivatives **6a,b**, and **9**, respectively.

*4.1.1.1. 4-Acetamido-N-(2,6-dioxopiperidin-3-yl)benzamide (**6a**).*

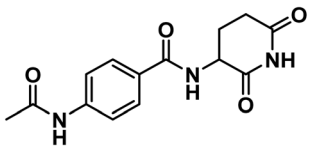

White crystal (yield, 75%); m.p. = 245–247 °C. IR (KBr, cm^{-1}): 3329, 3176 (NH), 3090 (CH aromatic), 2975 (CH aliphatic), 1693 (C=O imide), 1645 (C=O amide).; ^{1}H NMR (DMSO-d_6) δppm: 10.85 (s, 1H, CONHCO), 10.18 (s, 1H, CH_3CONH), 8.64 (d, J = 8 Hz, 1H, PhCONH), 7.84 (d, J = 8.2 Hz, 2H, Ar–H), 7.68 (d, J = 8.2 Hz, 2H, Ar–H), 4.78 (*m*, 1H, CH-piperidine), 2.80 (*m*, 1H, CHCONH-piperidine), 2.55 (*m*, 1H, CHCONH-piperidine), 2.15 (*m*, 1H, CHCH_2CONH-piperidine), 2.08 (s, 3H, CH_3), 1.97 (*m*, 1H, CHCH_2CONH-piperidine); mass (*m*/*z*): 289 (M^+, 31%), and 75 (100%, base peak); ^{13}C NMR (101 MHz, DMSO-d_6) δ 173.55, 172.82, 169.23, 166.07, 142.62, 128.68, 128.60, 118.56, 49.95, 31.48, 24.73, 24.59; Anal. Calcd. for $C_{14}H_{15}N_3O_4$ (289.29): C, 58.13; H, 5.23; N, 14.53. Found: C, 58.41; 5.40; N, 14.61%.

*4.1.1.2. N-(2,6-Dioxopiperidin-3-yl)-4-propionamidobenzamide (**6b**).*

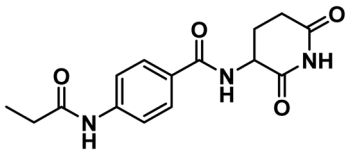

Grayish white crystal (yield, 67%); m.p. = 260–262 °C. IR (KBr, cm^{-1}): 3263, 3194 (NH), 3106 (CH aromatic), 2980 (CH aliphatic), 1728 (C=O imide), 1680 (C=O amide); ^{1}H NMR (DMSO-d_6) δppm: 10.84 (s, 1H, CONHCO), 10.11 (s, 1H, CH_2-CONH), 8.63 (d, J = 8.2 Hz, 1H, PhCONH), 7.83 (d, J = 8.4 Hz, 2H, Ar–H), 7.69 (d, J = 8.4 Hz, 2H, Ar–H), 4.77 (*m*, 1H, CH-piperidine), 2.80 (*m*, 1H, CH_2CH_2CONH-piperidine), 2.57 (*m*, 1H, CH_2CH_2CONH-piperidine), 2.36 (q, J = 7.5 Hz, 2H, CH_3-CH_2CO), 2.12 (*m*, 1H, CH_2CH_2CONH-piperidine), 1.98 (*m*, 1H, CH_2CH_2CONH-piperidine), 1.09 (t, J = 7.5 Hz, 3H, CH3); mass (*m*/*z*): 303 (M^+, 100%, base peak); ^{13}C NMR (101 MHz, DMSO-d_6) δ 173.53, 172.86, 172.81, 166.02, 142.67, 128.66, 128.48, 118.56, 49.91, 31.48, 30.04, 24.73, 9.97; Anal. Calcd. for $C_{15}H_{17}N_3O_4$ (303.32): C, 59.40; H, 5.65; N, 13.85. Found: C, 59.63; H, 5.81; N, 13.97%.

*4.1.1.3. 4-Benzamido-N-(2,6-dioxopiperidin-3-yl)benzamide (**9**).*

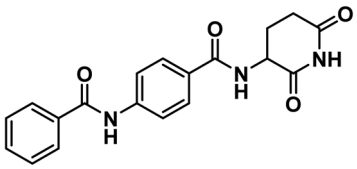

White crystal (yield, 75%); m.p. = 295–298 °C. IR (KBr, cm^{-1}): 3626, 3298 (2NH), 3098 (CH aromatic), 2923 (CH aliphatic), 1724 (C=O imide), 1647 (C=O amide); ^{1}H NMR (DMSO-d_6) δppm: 10.85 (s, 1H, CONHCO), 10.49 (s, 1H, PhCONHPh), 8.70 (d, J = 8.2 Hz, 1H, PhCONH), 7.98 (*m*, 2H, Ar–H), 7.91 (d, J = 8.2 Hz, 4H, Ar–H), 7.62 (*m*, 1H, Ar–H), 7.55 (*m*, 2H, Ar–H), 4.79 (*m*, 1H, CH-piperidine), 2.81 (*m*, 1H, CH_2CH_2CONH-piperidine), 2.56 (*m*, 1H, CH_2CH_2CONH-piperidine),2.14 (*m*, 1H, CH_2CH_2-CONH-piperidine), 2.01 (*m*, 1H, CH_2CH_2CONH-piperidine); ^{13}C NMR (101 MHz, DMSO-d_6) δ 173.54, 172.81, 166.32, 166.06, 142.55, 135.15, 132.27, 129.20, 128.91, 128.55, 128.23, 119.91, 49.96, 31.49, 24.75; Anal. Calcd. for $C_{19}H_{17}N_3O_4$ (351.36): C, 64.95; H, 4.88; N, 11.96. Found: C, 65.18; H, 4.96; N, 12.19%.

4.1.2. General procedure for synthesis of compound 12. Compound **12** was prepared in a similar manner of preparation of compounds **6a,b** in which a solution of compound **11** (1.00

 © 2023 The Author(s). Published by the Royal Society of Chemistry

Open Access Article. Published on 03 April 2023. Downloaded on 10/28/2025 2:01:20 AM.
This article is licensed under a Creative Commons Attribution-NonCommercial 3.0 Unported Licence.

mmol) and Et_3N (0.18 mL, 1.20 mmol) in DCM was treated with ethyl chloroformate (0.10 mL, 1.05 mmol). Then a solution of 3-aminopiperidine-2,6-dione HCl (0.17 g, 1.00 mmol) and triethyl amine (0.18 mL, 1.20 mmol) in DCM was added to the reaction mixture. The obtained solid was collected by filtration and recrystallized from ethanol to give the corresponding thioureidobenzamide derivative **12**, respectively.

*4.1.2.1. N-(2,6-Dioxopiperidin-3-yl)-4-(3-ethylthioureido) benzamide (**12**).*

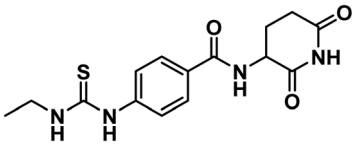

Yellow crystal (yield, 69%); m.p. = 220–222 °C. IR (KBr, cm^{-1}): 3752, 3652, 3314 (3NH), 3100 (CH aromatic), 2972 (CH aliphatic), 1726 (C=O imide), 1644 (C=O amide); ^{1}H NMR (DMSO-d_6) δppm: 10.85 (s, 1H, CONHCO), 9.68 (s, 1H, CSNHPh), 8.66 (d, J = 8.2 Hz, 1H, PhCONH), 7.95 (s, 1H, CH_2-NHCS), 7.82 (d, J = 8.4 Hz, 2H, Ar–H), 7.58 (d, J = 8.4 Hz, 2H, Ar–H), 4.77 (*m*, 1H, CH-piperidine), 3.49 (q, J = 6.8 Hz, 2H, CH_3-CH_2NH), 2.80 (*m*, 1H, CH_2CH_2CONH-piperidine), 2.57 (*m*, 1H, CH_2CH_2CONH-piperidine), 2.13 (*m*, 1H, CH_2CH_2CONH-piperidine), 1.99 (*m*, 1H, CH_2CH_2CONH-piperidine), 1.14 (t, J = 7.2 Hz, 3H, CH_3); ^{13}C NMR (101 MHz, DMSO-d_6) δ 180.40, 173.53, 172.77, 166.04, 142.97, 129.05, 128.33, 49.94, 39.15, 31.47, 24.73, 14.49; Anal. Calcd. for $C_{15}H_{18}N_4O_3S$ (334.11): C, 53.88; H, 5.43; N, 16.76. Found: C, 53.72; H, 5.49; N, 16.98%.

4.1.3. General procedure for synthesis of compounds 18a–g. A mixture of the appropriate potassium salt of substituted-2-mercaptoquinazoline-4(3H)-one **15a–g** (0.90 mmol), 2-chloro-*N*-(2,6-dioxopiperidin-3-yl)acetamide 17 (0.20 g, 0.99 mmol) and KI (catalytic amount) was stirred at r.t. for about 2 h in acetonitrile (15 mL). The obtained precipitates were collected by filtration, washed with water, dried, and crystallized from ethanol to afford the corresponding thioacetamide derivatives **18a–g**, respectively.

*4.1.3.1. 2-((5-Chloro-3-ethyl-4-oxo-3,4-dihydroquinazolin-2-yl) thio)-N-(2,6-dioxopiperidin-3-yl)acetamide (**18a**).*

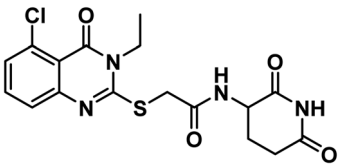

White crystal (yield, 74%); m.p. = 218–220 °C. IR (KBr, cm^{-1}): 3530, 3271 (2NH), 3085 (C–H aromatic), 2981 (C–H aliphatic), 1711 (C=O imide), 1680 (C=O amide) and 11 650 (amide II band); ^{1}H NMR (DMSO-d_6) δppm: 10.84 (s, 1H, CONHCO), 8.63 (d, J = 8.0 Hz, 1H, CONHCH), 7.68 (t, J = 8.0 Hz, 1H, Ar–H), 7.51 (d, J = 8.2 Hz, 1H, Ar–H), 7.45 (d, J = 7.8 Hz, 1H, Ar–H), 4.60 (*m*, 1H, CH-piperidine), 4.09 (q, J = 7.2 Hz, 2H, CH_2CH_3), 4.07 (s, 2H, SCH_2), 2.71 (*m*, 1H, CH_2CO-piperidine), 2.47 (*m*, 1H, CH_2CO-piperidine), 1.93 (*m*, 2H, CH_2CH-piperidine), 1.30 (t, J = 7 Hz, 3H, CH_3); mass (*m*/*z*): 408 (M^+, 16%), and 241 (100%, base peak); ^{13}C NMR (101 MHz, DMSO-d_6) δ 173.33, 172.42, 167.20, 158.59, 157.25, 149.56, 134.78, 133.03, 128.74, 126.12, 116.15, 50.06, 35.87, 31.26, 24.75, 13.21; Anal. Calcd. for $C_{17}H_{17}ClN_4O_4S$ (408.86): C, 49.94; H, 4.19; N, 13.70. Found: C, 49.71; H, 4.27; N, 13.96%.

*4.1.3.2. 2-((8-Chloro-3-ethyl-4-oxo-3,4-dihydroquinazolin-2-yl) thio)-N-(2,6-dioxopiperidin-3-yl)acetamide (**18b**).*

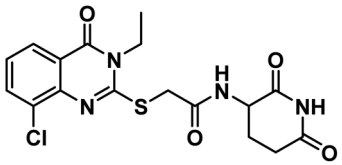

White crystal (yield, 74%); m.p. = 232–234 °C. IR (KBr, cm^{-1}): 3393, 3170 (2NH), 3083 (C–H aromatic), 2939 (C–H aliphatic), 1708 (C=O imide), 1679 (C=O amide) and 1646 (amide II band); ^{1}H NMR (DMSO-d_6) δppm: 10.82 (s, 1H, CONHCO), 8.63 (d, J = 8.0 Hz, 1H, CONHCH), 8.03 (dd, J = 8.0,1.5 Hz, 1H, Ar–H), 7.92 (dd, J = 7.8, 1.4 Hz, 1H, Ar–H), 7.42 (t, J = 7.9 Hz, 1H, Ar–H), 4.58 (*m*, 1H, CH-piperidine), 4.18 (q, J = 7.8 Hz, 2H, CH_2CH_3), 4.13 (s, 2H, SCH_2), 2.71 (*m*, 1H, CH_2CO-piperidine), 2.46 (*m*, 1H, CH_2CO-piperidine), 1.94 (*m*, 2H, CH_2CH-piperidine), 1.31 (t, J = 7.1 Hz, 3H, CH_3); ^{13}C NMR (101 MHz, DMSO-d_6) δ 173.35, 172.33, 166.78, 160.22, 157.76, 143.51, 134.93, 129.82, 126.61, 125.89, 120.83, 50.15, 36.10, 31.26, 24.62, 13.25; Anal. Calcd. for $C_{17}H_{17}ClN_4O_4S$ (408.86): C, 49.94; H, 4.19; N, 13.70. Found: C, 49.86; H, 4.31; N, 13.98%.

*4.1.3.3. N-(2,6-dioxopiperidin-3-yl)-2-((3-ethyl-5-fluoro-4-oxo-3,4-dihydroquinazolin-2-yl)thio)acetamide (**18c**).*

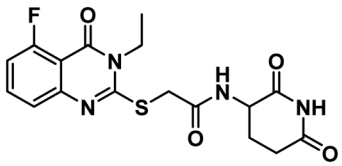

Shine yellow crystal (yield, 72%); m.p. = 252–250 °C. IR (KBr, cm^{-1}): 3273, 3210 (2NH), 3114 (C–H aromatic), 2978 (C–H aliphatic), 1720 (C=O imide), 1681 (C=O amide) and 1653 (amide II band); ^{1}H NMR (DMSO-d_6) δppm: 10.84 (s, 1H, CONHCO), 8.63 (d, J = 8.0 Hz, 1H, CONHCH), 7.74 (t, J = 8.0 Hz, 1H, Ar–H), 7.38 (d, J = 8.2 Hz, 1H, Ar–H), 7.18 (d, J = 7.8 Hz, 1H, Ar–H), 4.60 (*m*, 1H, CH-piperidine), 4.09 (q, J = 7.2 Hz, 2H, CH_2CH_3), 4.06 (s, 2H, SCH_2), 2.71 (*m*, 1H, CH_2CO-piperidine), 2.47 (*m*, 1H, CH_2CO-piperidine), 1.93 (*m*, 2H, CH_2CH-piperidine), 1.29 (t, J = 7.0 Hz, 3H, CH_3); mass (*m*/*z*): 392 (M^+, 3%), and 42 (100%, base peak); ^{13}C NMR (101 MHz, DMSO-d_6) δ 173.34, 172.42, 167.19, 162.17, 159.55, 157.65, 157.61, 149.10, 135.71, 135.61, 122.60, 122.56, 112.76, 112.56, 108.85, 50.05, 35.99, 31.26, 24.75, 13.27; Anal. Calcd. for $C_{17}H_{17}FN_4O_4S$ (392.41): C, 52.03; H, 4.37; N, 14.28. Found: C, 52.29; H, 4.50; N, 14.47%.

Open Access Article. Published on 03 April 2023. Downloaded on 10/28/2025 2:01:20 AM. This article is licensed under a Creative Commons Attribution-NonCommercial 3.0 Unported Licence.

*4.1.3.4. N-(2,6-Dioxopiperidin-3-yl)-2-((3-ethyl-6-fluoro-4-oxo-3,4-dihydroquinazolin-2-yl)thio)acetamide (**18d**).*

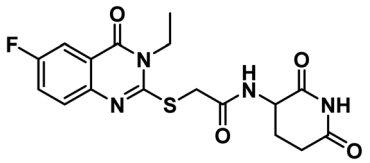

Shine yellow crystal (yield, 72%); m.p. = 227–229 °C. IR (KBr, cm^{-1}): 3301, 3169 (2NH), 3108 (C–H aromatic), 2954 (C–H aliphatic), 1713 (C=O imide), 1647 (C=O amide) and 1649 (amide II band); ^{1}H NMR (DMSO-d_6) δppm: 10.84 (s, 1H, CONHCO), 8.69 (d, J = 7.9 Hz, 1H, CONHCH), 7.72 (d, J = 8.8 Hz, 1H, Ar–H), 7.66 (d, J = 7.9 Hz, 1H, Ar–H), 7.64 (s, 1H, Ar–H), 4.60 (*m*, 1H, CH-piperidine), 4.11 (q, J = 7.2 Hz, 2H, CH_2CH_3), 4.07 (s, 2H, SCH_2), 2.71 (*m*, 1H, CH_2CO-piperidine), 2.46 (*m*, 1H, CH_2CO-piperidine), 1.94 (*m*, 2H, CH_2CH-piperidine), 1.30 (t, J = 7.0 Hz, 3H, CH_3); ^{13}C NMR (101 MHz, DMSO-d_6) δ 173.35, 172.42, 167.25, 161.05, 160.19, 158.63, 155.77, 144.21, 129.30, 129.22, 123.64, 123.40, 120.38, 120.30, 111.41, 111.17, 50.04, 35.95, 31.26, 24.74, 13.37; Anal. Calcd. for $C_{17}H_{17}FN_4O_4S$ (392.41): C, 52.03; H, 4.37; N, 14.28. Found: C, 52.79; H, 3.68; N, 14.04%.

*4.1.3.5. 2-((3-Allyl-5-chloro-4-oxo-3,4-dihydroquinazolin-2-yl) thio)-N-(2,6-dioxo piperidin-3-yl)acetamide (**18e**).*

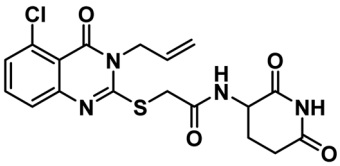

White crystal (yield, 71%); m.p. = 289–291 °C. IR (KBr, cm^{-1}): 3304, 3201 (2NH), 3093 (C–H aromatic), 2987 (C–H aliphatic), 1713 (C=O imide), 1684 (C=O amide) and 1645 (amide II band); ^{1}H NMR (DMSO-d_6) δppm: 10.84 (s, 1H, CONHCO), 8.61 (d, J = 8.0 Hz, 1H, CONHCH), 7.70 (t, J = 8.0 Hz, 1H, Ar–H), 7.53 (d, J = 8.2 Hz, 1H, Ar–H), 7.47 (d, J = 7.8 Hz, 1H, Ar–H), 5.93 (*m*, 1H, CH_2CHCH_2), 5.21 (*m*, 2H, CH_2CHCH_2), 4.68 (d, J = 5.1 Hz, 2H, NCH_2), 4.59 (*m*, 1H, CH-piperidine), 4.05 (s, 2H, SCH_2), 2.71 (*m*, 1H, CH_2CO-piperidine), 2.46 (*m*, 1H, CH_2CO-piperidine), 1.92 (*m*, 2H, CH_2CH-piperidine); mass (*m*/*z*): 420 (M^+, 23%), and 364 (100%, base peak);. ^{13}C NMR (101 MHz, DMSO-d_6) δ 173.33, 172.42, 167.16, 158.59, 157.69, 149.57, 134.94, 133.14, 131.62, 128.84, 126.18, 118.21, 116.09, 50.05, 46.58, 36.01, 31.26, 24.75; Anal. Calcd. for $C_{18}H_{17}ClN_4O_4S$ (420.87): C, 54.35; H, 4.32; N, 10.01. Found: C, 54.60; H, 4.41; N, 10.28%.

4.1.4. 2-((3-Allyl-6-chloro-4-oxo-3,4-dihydroquinazolin-2-yl) thio)-*N*-(2,6-dioxopiperidin-3-yl)acetamide (18f).

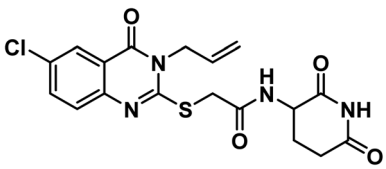

White crystal (yield, 71%); m.p. = 289–291 °C. IR (KBr, cm^{-1}): 3305, 3189 (2NH), 3086 (C–H aromatic), 2927 (C–H aliphatic), 1712 (C=O imide), 1678 (C=O amide) and 1628 (amide II band); ^{1}H NMR (DMSO-d_6) δppm: 10.83 (s, 1H, CONHCO), 8.62 (s, 1H, CONHCH), 7.99 (s, 1H, Ar–H), 7.81 (s, 1H, Ar–H), 7.60 (s, 1H, Ar–H), 5.92 (*m*, 1H, CH_2CHCH_2), 5.22 (*m*, 2H, CH_2CHCH_2), 4.72 (d, J = 5.2 Hz, 2H, NCH_2), 4.59 (*m*, 1H, CH-piperidine), 4.05 (s, 2H, SCH_2), 2.70 (*m*, 1H, CH_2CO-piperidine), 2.46 (*m*, 1H, CH_2CO-piperidine), 1.92 (*m*, 2H, CH_2CH-piperidine); ^{13}C NMR (126 MHz, DMSO-d_6) δ 172.71, 171.79, 166.59, 159.31, 156.93, 145.42, 134.72, 131.02, 129.94, 128.21, 125.28, 119.85, 117.71, 49.56, 35.59, 30.71, 24.19; Anal. Calcd. for $C_{18}H_{17}ClN_4O_4S$ (420.87): C, 54.35; H, 4.32; N, 10.01. Found: C, 54.56; H, 4.49; N, 10.02%.

4.1.5. 2-((3-Allyl-5-fluoro-4-oxo-3,4-dihydroquinazolin-2-yl) thio)-*N*-(2,6-dioxopiperidin-3-yl)acetamide (18g).

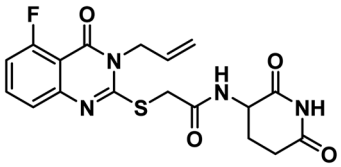

White crystal (yield, 71%); m.p. = 289–291 °C. IR (KBr, cm^{-1}): 3308, 3191 (2NH), 3092 (C–H aromatic), 2987 (C–H aliphatic), 1690 (C=O imide), 1623 (C=O amide) and 1640 (amide II band); ^{1}H NMR (DMSO-d_6) δppm: 10.84 (s, 1H, CONHCO), 8.62 (d, J = 8.0 Hz, 1H, CONHCH), 7.76 (t, J = 8.0 Hz, 1H, Ar–H), 7.40 (d, J = 8.2 Hz, 1H, Ar–H), 7.19 (d, J = 8.1 Hz, 1H, Ar–H), 5.92 (*m*, 1H, CH_2CHCH_2), 5.21 (*m*, 2H, CH_2CHCH_2), 4.69 (d, J = 5.1 Hz, 2H, NCH_2), 4.60 (*m*, 1H, CH-piperidine), 4.05 (s, 2H, SCH_2), 2.71 (*m*, 1H, CH_2CO-piperidine), 2.47 (*m*, 1H, CH_2CO-piperidine), 1.93 (*m*, 2H, CH_2CH-piperidine); ^{13}C NMR (126 MHz, DMSO-d_6) δ 172.72, 171.78, 166.58, 161.41, 159.32, 157.48, 148.55, 135.30, 131.12, 122.11, 117.62, 112.29, 108.21, 49.53, 45.58, 35.60, 30.70, 24.18; Anal. Calcd. for $C_{18}H_{17}FN_4O_4S$ (404.42): C, 56.57; H, 4.50; N, 10.42. Found: C, 56.78; H, 4.62; N, 10.68%.

4.1.6. General procedure for synthesis of compounds (21a–c). A mixture of an appropriate potassium salt of 2-mercaptoquinazolin-4-one derivative **15a,f**, and **g** (0.90 mmol) and 2-chloro-*N*-(3-chloro-4-fluorophenyl)acetamide **20** (0.20 g, 0.90 mmol) was stirred at r.t. in acetonitrile for about **2h** in presence of catalytic amount of KI. The obtained precipitates were filtered off and crystallized from ethanol to furnish the corresponding thioacetamide products **21a–c**.

*4.1.6.1. 2-((5-Chloro-3-ethyl-4-oxo-3,4-dihydroquinazolin-2-yl) thio)-N-(3-chloro-4-fluorophenyl)acetamide (**21a**).*

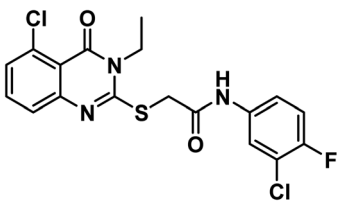

Off white crystal (yield, 85%); m.p. = 240–244 °C. IR (KBr, cm^{-1}): 3257 (NH), 3044 (C–H aromatic), 2987 (C–H

 © 2023 The Author(s). Published by the Royal Society of Chemistry

Open Access Article. Published on 03 April 2023. Downloaded on 10/28/2025 2:01:20 AM. This article is licensed under a Creative Commons Attribution-NonCommercial 3.0 Unported Licence.

aliphatic), 1669 (C=O amide) and 1643 (amide II band); ^{1}H NMR (DMSO-d_6) δppm: 10.69 (s, 1H, NH), 7.92 (s, 1H, Ar–H), 7.67 (t, J = 8.0 Hz, 1H, Ar–H), 7.52 (s, 1H, Ar–H), 7.44 (m, 1H, Ar–H), 7.37 (m, 2H, Ar–H), 4.21 (s, 2H, SCH_2), 4.08 (q, J = 7.4 Hz, 2H, NCH_2CH_3), 1.31 (t, J = 7.0 Hz, 3H, CH_3); MS (m/z): 428 (M^++1, 34%), 426 (M^+, 52%), 147 (100%, base peak); ^{13}C NMR (101 MHz, DMSO-d_6) δ 166.53, 158.53, 157.30, 154.80, 152.39, 149.48, 136.82, 134.88, 133.12, 128.79, 125.86, 120.94, 119.91, 119.51, 117.37, 116.16, 36.98, 13.22; Anal. Calcd. for $C_{18}H_{14}Cl_2FN_3O_2S$ (426.29): C, 50.72; H, 3.31; N, 9.86. Found: C, 50.97; H, 3.45; N, 9.98%.

*4.1.6.2. 2-((6-Chloro-3-ethyl-4-oxo-3,4-dihydroquinazolin-2-yl)thio)-N-(3-chloro-4-fluorophenyl)acetamide (**21b**).*

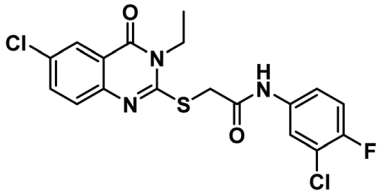

Grayish white crystal (yield, 85%); m.p. = 209–211 °C. IR (KBr, cm^{-1}): 3251 (NH), 3049 (C–H aromatic), 2985 (C–H aliphatic), 1675 (C=O amide) and 1619 (amide II band); ^{1}H NMR (DMSO-d_6) δppm: 10.61 (s, 1H, NH), 7.91 (s, 1H, Ar–H), 7.71 (s, Hz, 1H, Ar–H), 7.50(m, 1H, Ar–H), 7.38 (d, J = 7.6 Hz, 1H, Ar–H), 7.19 (s, 2H, Ar–H), 4.20 (s, 2H, SCH_2), 4.08 (q, J = 7.1 Hz, 2H, NCH_2CH_3), 1.29 (t, J = 7.1 Hz, 3H, CH_3); ^{13}C NMR (101 MHz, DMSO-d_6) δ 166.51, 159.75, 157.10, 154.81, 152.40, 145.86, 136.81, 135.25, 130.41, 128.45, 125.77, 120.95, 120.48, 119.85, 119.52, 117.37, 37.09, 13.33; Anal. Calcd. for $C_{18}H_{14}ClF_2N_3O_2S$ (409.84): C, 52.75; H, 3.44; N, 10.25. Found: C, 52.91; H, 3.63; N, 10.12%.

*4.1.6.3. N-(3-chloro-4-fluorophenyl)-2-((3-ethyl-5-fluoro-4-oxo-3,4-dihydroquinazolin-2-yl)thio)acetamide (**21c**).*

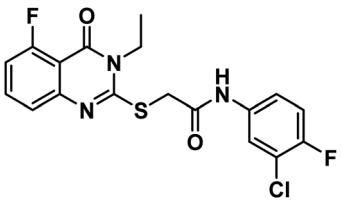

White crystal (yield, 82%); m.p. = 279–281 °C. IR (KBr, cm^{-1}): 3262 (NH), 3063 (C–H aromatic), 2987 (C–H aliphatic), 1686 (C=O amide) and 1652 (amide II band); ^{1}H NMR (DMSO-d_6) δppm: 10.74 (s, 1H, NH), 8.0 (s, 1H, Ar–H), 7.92 (s, Hz, 1H, Ar–H), 7.80 (dd, J = 8.7, 2.6 Hz, 1H, Ar–H), 7.52 (d, J = 7.6 Hz, 1H, Ar–H), 7.46 (d, J = 8.7 Hz, 1H, Ar–H), 7.39 (t, J = 9.1 Hz, 1H, Ar–H), 4.23 (s, 2H, SCH_2), 4.13 (q, J = 7.1 Hz, 2H, NCH_2CH_3), 1.31 (t, J = 7.1 Hz, 3H, CH_3); ^{13}C NMR (126 MHz, DMSO-d_6) δ 166.06, 161.60, 159.51, 157.29, 154.27, 152.34, 148.66, 136.31, 135.42, 121.89, 120.68, 119.54, 117.22, 112.27, 108.49, 39.44, 36.75, 12.90. Anal. Calcd. for $C_{18}H_{14}Cl_2FN_3O_2S$ (426.29): C, 50.72; H, 3.31; N, 9.86. Found: C, 50.99; H, 3.48; N, 9.93%.

4.2. Biological testing

4.2.1. *In vitro* antitumor assay. This test was carried out on three different human cancer cell lines: MCF-7, HCT116, and HepG-2 using the MTT method[32–34] as described in ESI.†

4.2.2. Estimation of TNF-α, CASP8, and VEGF in HepG-2 cells supernatant. The levels of TNF-α, CASP8, and VEGF in cell culture supernatants were estimated by ELISA technique using commercially available matched paired antibodies (R&D Systems Inc., Minneapolis, MN) according to reported procedure[35,36] as described in ESI.†

4.2.3. Estimation of nuclear factor kappa-B P65 (NF-κB P65) in HepG-2 cell lysate. Anti-rabbit NF-κB P65 polyclonal antibody was measured using the ELISA plate reader in cell lysate[37] as described in ESI.†

4.2.4. Flow cytometry analysis for cell cycle. Cell cycle analysis was performed using propidium iodide (PI) staining and flow cytometry analysis for compound **12l** as described in ESI†.[38,39]

4.2.5. Flow cytometry analysis for apoptosis. Apoptotic effect was assessed for compound **12l** as described in ESI†.[40,41]

4.2.6. *In silico* studies

4.2.6.1. ADMET studies. ADMET descriptors were determined using Discovery studio 4.0 as according to the reported method[42–45] (ESI†).

4.2.6.2. Toxicity studies. The toxicity parameters of the synthesized compounds were calculated using Discovery studio 4.0 as described[46–49] in ESI.†

Conflicts of interest

There is no conflict of interest.

Acknowledgements

This paper is based upon work supported by Science, Technology & Innovation Funding Authority (STIFA) under grant number 43040.

References

1 A. A. Gaber, A. H. Bayoumi, A. M. El-Morsy, F. F. Sherbiny, A. B. Mehany and I. H. Eissa, *Bioorg. Chem.*, 2018, **80**, 375–395.
2 R. A. Asherson, K. Gunter, D. Daya and Y. Shoenfeld, *J. Rheumatol.*, 2008, **35**, 1224–1227.
3 L. S. Chan, *Clin. Dermatol.*, 2012, **30**, 34–37.
4 A. Mercurio, G. Adriani, A. Catalano, A. Carocci, L. Rao, G. Lentini, M. M. Cavalluzzi, C. Franchini, A. Vacca and F. Corbo, *Curr. Med. Chem.*, 2017, **24**, 2736–2744.
5 S. Joglekar and M. Levin, *Drugs Today*, 2004, **40**, 197–204.
6 R. Knight, *Seminars in Oncology*, Elsevier, 2005, pp. 24–30.
7 J. Folkman, *Seminars in Oncology*, Elsevier, 2001, pp. 536–542.
8 M. Melchert and A. List, *Int. J. Biochem. Cell Biol.*, 2007, **39**, 1489–1499.

Open Access Article. Published on 03 April 2023. Downloaded on 10/28/2025 2:01:20 AM.
This article is licensed under a Creative Commons Attribution-NonCommercial 3.0 Unported Licence.

9 A. L. Ruchelman, H.-W. Man, W. Zhang, R. Chen, L. Capone, J. Kang, A. Parton, L. Corral, P. H. Schafer and D. Babusis, *Bioorg. Med. Chem. Lett.*, 2013, **23**, 360–365.
10 S. K. Teo, *AAPS J.*, 2005, **7**, E14–E19.
11 R. Suppiah, J. G. Srkalovic and M. A. Hussein, *Clin. Lymphoma Myeloma*, 2006, **6**, 301–305.
12 E. Terpos, N. Kanellias, D. Christoulas, E. Kastritis and M. A. Dimopoulos, *OncoTargets Ther.*, 2013, **6**, 531.
13 S. Singhal and J. Mehta, *Biomed. Pharmacother.*, 2002, **56**, 4–12.
14 J. B. Marriott, G. Muller and A. G. Dalgleish, *Immunol. Today*, 1999, **20**, 538–540.
15 T. Ito and H. Handa, *Proc. Jpn. Acad., Ser. B*, 2020, **96**, 189–203.
16 C. C. Bjorklund, J. Kang, M. Amatangelo, A. Polonskaia, M. Katz, H. Chiu, S. Couto, M. Wang, Y. Ren and M. Ortiz, *Leukemia*, 2020, **34**, 1197–1201.
17 L. Li, W. Xue, Z. Shen, J. Liu, M. Hu, Z. Cheng, Y. Wang, Y. Chen, H. Chang and Y. Liu, *Mol. Ther.-Oncolytics*, 2020, **18**, 215–225.
18 A. R. Kotb, D. A. Bakhotmah, A. E. Abdallah, H. Elkady, M. S. Taghour, I. H. Eissa and M. A. El-Zahabi, *RSC Adv.*, 2022, **12**, 33525–33539.
19 J. Qiu, B. Xu, Z. Huang, W. Pan, P. Cao, C. Liu, X. Hao, B. Song and G. Liang, *Bioorg. Med. Chem.*, 2011, **19**, 5352–5360.
20 A. E. Abdallah, M. S. Alesawy, S. I. Eissa, E. M. El-Fakharany, M. H. Kalaba, M. H. Sharaf, N. M. A. Shama, S. H. Mahmoud, A. Mostafa and A. A. Al-Karmalawy, *New J. Chem.*, 2021, **45**, 16557–16571.
21 A. E. Abdallah, R. R. Mabrouk, M. M. S. Al Ward, S. I. Eissa, E. B. Elkaeed, A. B. Mehany, M. A. Abo-Saif, O. A. El-Feky, M. S. Alesawy and M. A. El-Zahabi, *J. Enzyme Inhib. Med. Chem.*, 2022, **37**, 573–591.
22 A. S. El-Azab, A. A.-M. Abdel-Aziz, H. A. Ghabbour and M. A. Al-Gendy, *J. Enzyme Inhib. Med. Chem.*, 2017, **32**, 1229–1239.
23 A. E. Abdallah, S. I. Eissa, M. M. S. Al Ward, R. R. Mabrouk, A. B. Mehany and M. A. El-Zahabi, *Bioorg. Chem.*, 2021, **109**, 104695.
24 F. Bray, J. Ferlay, I. Soerjomataram, R. L. Siegel, L. A. Torre and A. Jemal, *Ca-Cancer J. Clin.*, 2018, **68**, 394–424.
25 E. B. Elkaeed, R. G. Yousef, H. Elkady, A. B. Mehany, B. A. Alsfouk, D. Z. Husein, I. M. Ibrahim, A. M. Metwaly and I. H. Eissa, *J. Biomol. Struct. Dyn.*, 2022, 1–16.
26 M. S. Taghour, H. Elkady, W. M. Eldehna, N. El-Deeb, A. M. Kenawy, E. B. Elkaeed, B. A. Alsfouk, M. S. Alesawy, D. Z. Husein and A. M. Metwaly, *PLoS One*, 2022, **17**, e0272362.
27 R. G. Yousef, H. Elkady, E. B. Elkaeed, I. M. Gobaara, H. A. Alghulikah, D. Z. Husein, I. M. Ibrahim, A. M. Metwaly and I. H. Eissa, *Molecules*, 2022, **27**, 7719.
28 E. B. Elkaeed, R. G. Yousef, H. Elkady, A. A. Alsfouk, D. Z. Husein, I. M. Ibrahim, M. Alswah, H. S. Elzahabi, A. M. Metwaly and I. H. Eissa, *Processes*, 2022, **10**, 2290.
29 N. A. Alsaif, M. A. Dahab, M. M. Alanazi, A. J. Obaidullah, A. A. Al-Mehizia, M. M. Alanazi, S. Aldawas, H. A. Mahdy and H. Elkady, *Bioorg. Chem.*, 2021, **110**, 104807.
30 S. A. El-Metwally, M. M. Abou-El-Regal, I. H. Eissa, A. B. Mehany, H. A. Mahdy, H. Elkady, A. Elwan and E. B. Elkaeed, *Bioorg. Chem.*, 2021, **112**, 104947.
31 N. A. Alsaif, M. S. Taghour, M. M. Alanazi, A. J. Obaidullah, A. A. Al-Mehizia, M. M. Alanazi, S. Aldawas, A. Elwan and H. Elkady, *J. Enzyme Inhib. Med. Chem.*, 2021, **36**, 1093–1114.
32 D. Gerlier and N. Thomasset, *J. Immunol. Methods*, 1986, **94**, 57–63.
33 A. I. Abd-Elhamid, H. El-Gendi, A. E. Abdallah and E. M. El-Fakharany, *Pharmaceutics*, 2021, **13**, 1595.
34 N. T. Dawoud, E. M. El-Fakharany, A. E. Abdallah, H. El-Gendi and D. R. Lotfy, *Sci. Rep.*, 2022, **12**, 1–17.
35 R. M. Talaat, *Viral Immunol.*, 2010, **23**, 151–157.
36 *MyBioSource ELISA Test Kits*, **https://www.mybiosource.com/human-elisa-kits/casp8/2513072#QLAPP_MBS2513072_TD**, (accessed May 2018).
37 M. A. El-Zahabi, H. Sakr, K. El-Adl, M. Zayed, A. S. Abdelraheem, S. I. Eissa, H. Elkady and I. H. Eissa, *Bioorg. Chem.*, 2020, **104**, 104218.
38 J. Wang and M. J. Lenardo, *J. Cell Sci.*, 2000, **113**, 753–757.
39 W. M. Eldehna, G. S. Hassan, S. T. Al-Rashood, T. Al-Warhi, A. E. Altyar, H. M. Alkahtani, A. A. Almehizia and H. A. Abdel-Aziz, *Med. Chem.*, 2019, **34**, 322–332.
40 K. K.-W. Lo, T. K.-M. Lee, J. S.-Y. Lau, W.-L. Poon and S.-H. Cheng, *Inorg. Chem.*, 2008, **47**, 200–208.
41 A. Sabt, O. M. Abdelhafez, R. S. El-Haggar, H. M. Madkour, W. M. Eldehna, E. E.-D. A. El-Khrisy, M. A. Abdel-Rahman and L. A. Rashed, *Med. Chem.*, 2018, **33**, 1095–1107.
42 E. B. Elkaeed, R. G. Yousef, H. Elkady, I. M. Gobaara, A. A. Alsfouk, D. Z. Husein, I. M. Ibrahim, A. M. Metwaly and I. H. Eissa, *Processes*, 2022, **10**, 1391.
43 E. B. Elkaeed, R. G. Yousef, H. Elkady, I. M. Gobaara, B. A. Alsfouk, D. Z. Husein, I. M. Ibrahim, A. M. Metwaly and I. H. Eissa, *Molecules*, 2022, **27**, 4606.
44 E. B. Elkaeed, I. H. Eissa, H. Elkady, A. Abdelalim, A. M. Alqaisi, A. A. Alsfouk, A. Elwan and A. M. Metwaly, *Int. J. Mol. Sci.*, 2022, **23**, 8407.
45 E. B. Elkaeed, F. S. Youssef, I. H. Eissa, H. Elkady, A. A. Alsfouk, M. L. Ashour, M. A. El Hassab, S. M. Abou-Seri and A. M. Metwaly, *Int. J. Mol. Sci.*, 2022, **23**, 6912.
46 M. S. Taghour, H. Elkady, W. M. Eldehna, N. M. El-Deeb, A. M. Kenawy, E. B. Elkaeed, A. A. Alsfouk, M. S. Alesawy, A. M. Metwaly and I. H. Eissa, *J. Enzyme Inhib. Med. Chem.*, 2022, **37**, 1903–1917.
47 A. Belal, N. M. Abdel Gawad, A. B. Mehany, M. A. Abourehab, H. Elkady, A. A. Al-Karmalawy and A. S. Ismael, *J. Enzyme Inhib. Med. Chem.*, 2022, **37**, 1884–1902.
48 M. M. Alanazi, H. Elkady, N. A. Alsaif, A. J. Obaidullah, H. M. Alkahtani, M. M. Alanazi, M. A. Alharbi, I. H. Eissa and M. A. Dahab, *RSC Adv.*, 2021, **11**, 30315–30328.
49 M. M. Alanazi, H. Elkady, N. A. Alsaif, A. J. Obaidullah, W. A. Alanazi, A. M. Al-Hossaini, M. A. Alharbi, I. H. Eissa and M. A. Dahab, *J. Mol. Struct.*, 2021, 132220.

 © 2023 The Author(s). Published by the Royal Society of Chemistry